OMAE2017-62159

A STUDY ON AN ICEBERG DRIFT TRAJECTORY

Leif Erik Andersson[*]
Department of Engineering Cybernetics
Norwegian University of Science and Technology
7491 Trondheim
Norway
Email: leif.e.andersson@ntnu.no

Francesco Scibilia
Statoil Research Center
Statoil ASA
7053 Ranheim
Norway
Email: fsci@statoil.com

Lars Imsland
Department of Engineering Cybernetics
Norwegian University of Science and Technology
7491 Trondheim
Norway
Email: lars.imsland@ntnu.no

ABSTRACT

Iceberg drift forecast is a challenging process. Large uncertainties in iceberg geometry and in the driving forces - current, wind and waves - make accurate forecasts difficult. This article illustrates from a data set that even if the uncertainties in current, wind and waves are reduced the forecast using a dynamic iceberg models stays difficult, because of the sensitivity of the model to different parameters and inputs. Nevertheless, if the uncertainty of the current driving force on the iceberg is reduced by measuring the current at the iceberg location, it is possible under specific conditions to estimate the approximate iceberg shape. This iceberg shape geometry can be used directly in the dynamic iceberg model.

NOMENCLATURE

a   Major axis of ellipse $[m]$
A   Iceberg layer cross sectional area $[m^2]$
b   Minor axis of ellipse $[m]$
$\mathbf{F_a}$ Air drag force $[N]$
$\mathbf{F_c}$ Water drag force $[N]$
$\mathbf{F_{cor}}$ Coriolis force $[N]$
$\mathbf{F_p}$ Pressure gradient force $[N]$
$\mathbf{F_r}$ Wave radiation force $[N]$
h   Iceberg layer height $[m]$
k   Ratio between minor and major axis $[-]$
m   Iceberg mass $[kg]$

p   Vector of parameters
r   Iceberg layer radius $[m]$
R   Measurement noise covariance $[-]$
u   Vector of inputs
v   Measurement noise
$\mathbf{V}$ Iceberg velocity $[m/s]$
V_{keel} Iceberg keel volume $[m^3]$
V_{sail} Iceberg sail volume $[m^3]$
x   Vector of differential states
y   Vector of outputs
ρ_{ice} Iceberg density $[kg/m^3]$
ρ_w Water density $[kg/m^3]$

INTRODUCTION

Icebergs are a threat to navigation and offshore installations. Good operational iceberg drift forecasts are important for marine operations such as station keeping in areas subjected to drifting icebergs. Mechanistic dynamic models, which model the drift of an iceberg by considering the forces that act on the iceberg, have been developed by [1–3]. An operational iceberg drift model was developed at the Canadian Ice Service [4]. The model uses environmental inputs as winds, waves and currents and detailed description of the iceberg keel geometry to simulate the iceberg trajectory.

Currents are usually identified as the most important driving force for the iceberg drift [4–7]. However, current direction and speed are identified as the most uncertain iceberg model param-

---

[*]Address all correspondence to this author.

eters. This introduces large uncertainties into the iceberg drift forecast [8]. Even if the main drift direction of the operational iceberg model is claimed to be satisfactory [3,4,9], the modelled and observed iceberg trajectories can deviate from the beginning and even point in different directions [2].

One of the most comprehensive iceberg drift data sets were collected by Smith and Donaldson [1] [10]. The dynamic model was able to represent the majority of the observed tracks reasonably. However, drag coefficients were optimized and wind corrected for their analysis. Furthermore, some observed tracks showed considerable deviation from the modelled track.

A new research effort lead by C-CORE developed and improved iceberg profiling. It is possible to profile the iceberg in relative short time [11] and use these profiles in Iceberg Management systems to prepare towing [12], model iceberg impacts [13] or evaluate the risk to sub sea installations [14, 15]. These iceberg profiles are collected by approaching the iceberg with a ship. Others work on profiling the iceberg sail and keel with underwater vehicles was undertaken [16, 17]. However, it is not straightforward to include a detailed 3D iceberg profile into the dynamic iceberg model.

In Spring 2015 ArticNet [18] and Statoil conducted an Offshore Newfoundland Researcher Expedition. During this expedition a data set of one iceberg track similar to the one collected by Smith and Donaldson [1] [10] was collected. This paper discusses the sensitivity of the dynamic iceberg model to different input signals and model parameters. Furthermore, it is shown how current data collected close to the iceberg can be used to improve knowledge about the iceberg shape without profiling the iceberg keel.

DATA COLLECTION

The iceberg discussed here was discovered during the Offshore Newfoundland Research Expedition on April 24th 2015.

The iceberg sail was measured to be about 30.5 m, the width 100 m and the length 281 m. The little attachment in front of the iceberg is not included into the iceberg length (Fig. 1). The iceberg has a form like an S-curved dumbbell. The width is approximated and is measured in the middle of the iceberg. Without a more precise overview of the iceberg, the side-pictures would suggest that the iceberg has a width of about 150 m to 190 m. The length and width of the iceberg are identified by the known sail height and a simple image-processing program. The keel depth was estimated with the ship-mounted SX90 sonar to be 90-100m.

The formulas available for calculating the iceberg draft based on waterline length overestimate the draft with 160m, 197m, 151m and 140 m [2] [19, 20]. The dumbbell shape of the
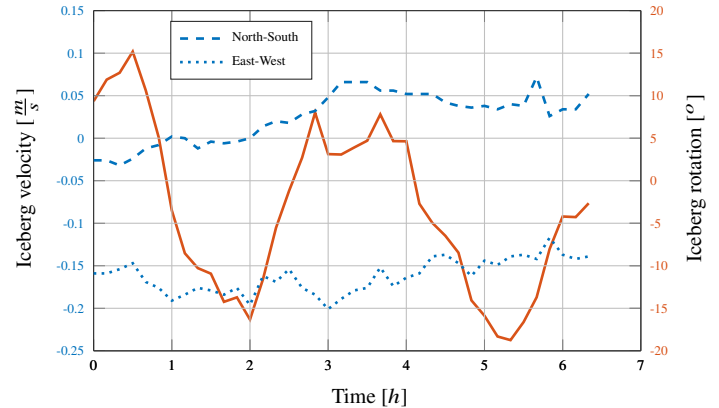

FIGURE 2: ICEBERG VELOCITY IN NORTH-SOUTH (DASHED) AND EAST-WEST (DOTTED) DIRECTIONS AND THE ROTATION OF THE ICEBERG (SOLID).

iceberg probably causes this. It is probable that only one "bell" is responsible for the keel depth while the other one has a smaller keel depth. The larger "bell" of the iceberg has a length of about 145 m, which results in an iceberg draft of about 96 m to 101 m using the formulas [2]. This is very close to the actual measured keel depth.

Four GPS beacons were deployed on the iceberg at around 15:15 UTC. The iceberg velocity and rotation is shown in Fig. 2. The velocity in north-south and east-west direction changes only slightly during the observation. The long axis of the iceberg rotates between $\pm 15°$ from the north direction. The period of this oscillation is about 3 h.

Between 14:20 and 21:50 UTC, a wave glider operated close to the iceberg. The wave glider collected wave, current, wind data. At the same time current data was collected from the icebreaker *Amundsen*, which stayed close to the iceberg (Fig. 3).

Wind information was available from the *Amundsen*, the wave glider (5 min frequency), manual observations (1 h frequency) on the *Amundsen* and from the weather forecast (6 h frequency). The automatic wind measurements on the *Amundsen* were excluded from the analyses, since they did not correlate with the other wind information. Therefore, it was assumed that they were error-prone and not trust-worthy (Fig. 4).

The current information was received by the Shipboard Acoustic Doppler Current Profiles (SADCP). The current profiles that are important for the iceberg are shown in Fig. 5. The layer size is 8 m. The centre of the first 8 m height bin is at 23.2 m. It is assumed that the surface current is similar to the current measured in the first bin. Because of the position of the sonar underneath the ship, it was not possible to measure currents closer to the surface. The current is measured with a 5 min frequency. The currents are similar in the current layers. Nevertheless, sometimes a direction change can be detected between near surface and deeper currents. Between hours 3 to 4 the cur-

---

[1] Current profiles and wind data were collected from twelve track segments of seven different icebergs. In addition, the mass and cross sectional areas were estimated based on sonar profiles and photographs.

[2] 1) $2.91L^{0.71}$, 2) $0.7L$, 3) $3.27L^{0.68}$, 4) $3.31L^{0.56}H^{0.17}$

(a) ICEBERG VIEW FROM ONE SIDE.

(b) ICEBERG VIEW FROM OPPOSITE SIDE.

(c) ICEBERG VIEW ON LONG SIDE.

FIGURE 1: ICEBERG FROM SEVERAL SIDES

rent measurements show strong peaks, which are probably several outliers (large errors in the current measurement). The overall current velocity is small.

The wave glider measured significant wave height and wave peak direction. The measurement frequency was 30 min. The waves propagate from south-east-east to north-west-west. Consequently, waves have a stronger westerly component, while a weaker northerly component (Fig. 6). In comparison, the wind blows from north-east-east to south-west-west. The average difference between wave and wind direction is 26°. The average wave height is 1.56 m and the average wind velocity 8.7 m/s.

ICEBERG DRIFT SIMULATION

In this section, the iceberg is simulated based on the measured forcing on the iceberg. The simulation period of 6.5 hours is quite short. However, some conclusion can be drawn anyway.

Iceberg model

The North-East-Down coordinate system is used in this article. The ocean is assumed a plane and the origin of the coordinate system is the initial position of the observed iceberg.

The iceberg model can be described by a set of ordinary differential equations (ODEs)

$$\dot{x} = f(x, u, p), \quad x_0 = x(t_0), \tag{1a}$$
$$y = h(x), \tag{1b}$$

where $x \in \mathbb{R}^{n_x}$ is the vector of differential states, $u \in \mathbb{R}^{n_u}$ the vector of inputs, $y \in \mathbb{R}^{n_y}$ the vector of outputs, and $p \in \mathbb{R}^{n_p}$ vector of parameters . For the iceberg model, x is the iceberg position and the velocity, u are the environmental driving forces, current, wind and waves, and y is the observed iceberg position.

More specifically, mechanistic dynamic iceberg models are based on a momentum equation to describe the change of velocity of the iceberg mass

$$m\frac{d\mathbf{V_i}}{dt} = \mathbf{F_{cor}} + \mathbf{F_a} + \mathbf{F_c} + \mathbf{F_r} + \mathbf{F_p}, \tag{2}$$

where m, $\mathbf{V_i}$, $\mathbf{F_{cor}}$, $\mathbf{F_a}$, $\mathbf{F_c}$, $\mathbf{F_r}$ and $\mathbf{F_p}$ are the iceberg mass, iceberg velocity, Coriolis force, the air drag force, the water drag force, the wave radiation force and pressure gradient term, respectively (Fig. 7). Bold symbols are used for two-dimensional vector quantities.

The approach was proposed in the seventies [21] and further developed and evaluated by many different authors, for example [3,5,10,22] and more recently [7]. For more details on the iceberg model used in this article, the reader is referred to [23].

Sensitivity of iceberg shape to different current measurements

Three different iceberg keel shapes are considered: A rectangular, a semi-elliptic and a triangular keel shape (Fig. 8). The mass is assumed constant and not changed together with the keel
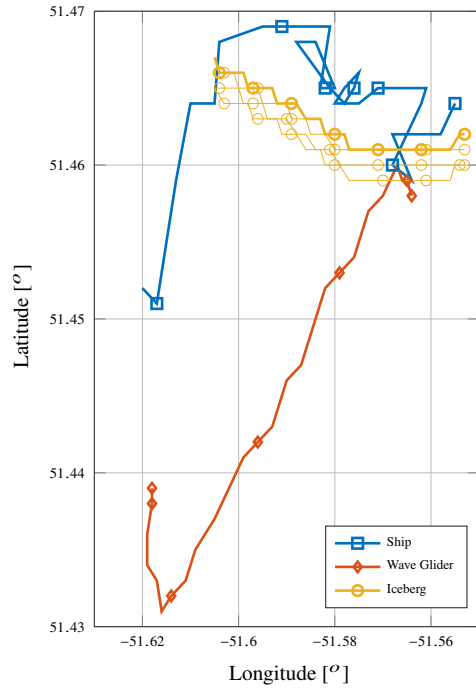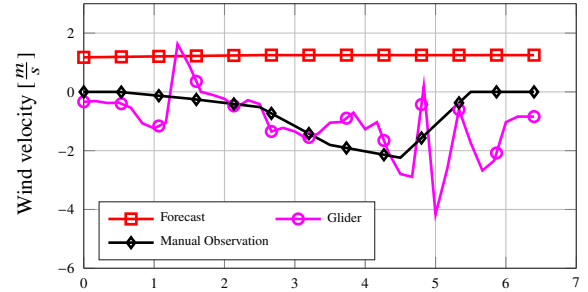
FIGURE 3: SHIP, GLIDER AND ICEBERG POSITION. EVERY HOUR IS A MARK SET INTO THE TRAJECTORY. THE POSITION OF FOUR GPS BEACONS ON THE ICEBERG IS SHOWN.
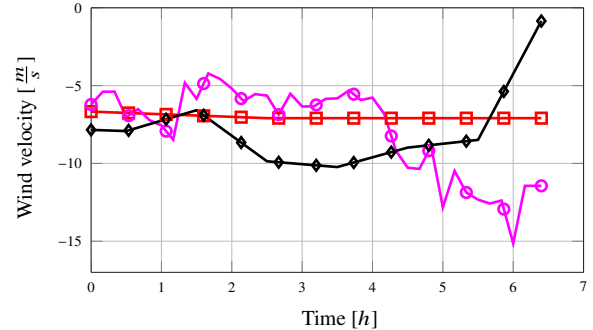

(a) NORTH-SOUTH VELOCITY

(b) EAST-WEST VELOCITY

FIGURE 4: WIND VELOCITY IN NORTH-SOUTH AND EAST-WEST DIRECTION. WIND DIRECTION IS POSITIVE IF IT BLOWS IN NORTH AND IN EAST DIRECTION.

shapes.

In the first simulation study the wave force is neglected. The initial iceberg velocity is calculated with the first two iceberg position measurements (Fig. 9). The three iceberg keel shapes behave considerably differently. The error between simulated and observed iceberg trajectory increases over the observation horizon for all three iceberg keel shapes. The triangular shaped iceberg keel shows the smallest and the rectangular shaped iceberg keel the largest error. The triangular shaped iceberg keel is more strongly influenced by the surface and near surface currents than the other iceberg shapes. Therefore, it can be concluded that the surface current layer is probably not weighted strong enough during the simulations with the rectangular and elliptical iceberg keel shape.

If only the surface current layer is used as current for the whole iceberg keel the error between observed iceberg trajectory and simulated iceberg trajectory reduces significantly compared to the results shown in Fig. 9. For this new configuration, the elliptic shaped iceberg keel produces the smallest error. The triangular shaped iceberg keel overestimates the east velocity of the iceberg compared to the other iceberg keel shapes. This is caused by the strong eastward wind velocity observed by the wave glider at the end of the observation horizon (Fig. 4).

The manual wind observations on the other hand shows a decrease in wind velocity. If the iceberg is simulated using the first current layer and the manual observed wind velocities, the rectangular shaped iceberg keel has the smallest final position error. This error is even smaller than the final error of the elliptic shaped iceberg using the wind velocities measured by the wave glider.

That is, all three geometries may behave best depending on which combination of input signals are used in the simulations.

Sensitivity of iceberg model to different input signals and geometry assumptions

In order to investigate further the influence of different input signals and the iceberg shape assumptions, every possible combination with the following variables were simulated:

1. Iceberg keel shape: Rectangular, Triangular, Semi-Elliptic
2. Current Input: Mean current, surface current, layered current
3. Wind Input: manual observed wind, wave glider wind, wind forecast
4. Wave Input: Included or Excluded
5. Pressure gradient force: Yes or No
6. Coriolis force: Yes or No.

Other parameters, like the drag coefficients, were not changed during these 216 iceberg drift simulations. The root-mean square error, final and maximum error of the drift hindcast were ana-
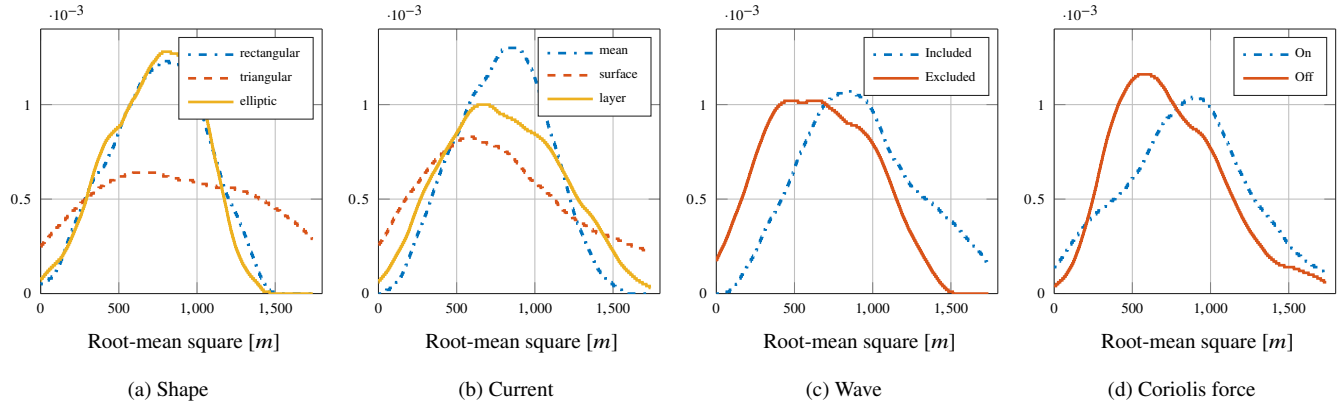
FIGURE 10: PROBABILITY DENSITY FUNCTION OF DIFFERENT PARAMETERS.

lyzed, first for each individual simulation option and afterwards for different combination of options.

The smallest root mean square error of 102 m is achieved by the combination: rectangular iceberg keel shape, surface current, manual observed wind, no waves, no pressure gradient force, but Coriolis force. The second best hindcast was achieved by switching on the pressure gradient force, which gave the root-mean square error of 178 m.

The largest root-mean square error was 1741 m and was caused by the combination: triangular iceberg shape, surface current, manual observed wind, waves, no pressure gradient force, but Coriolis force. A similar error was achieved with pressure gradient force. The difference to the best one is due to the iceberg shape and the wave force.

In a second step, the results were visualized by fitting the performance indices into a kernel distribution and plotting the resulting *probability density function* (pdf) (interpreting the mean square error from the different experiments as a random variable) (Fig. 10). It can be seen easily that the triangular shaped iceberg has a larger variance in the root mean square error. In addition, the mean is larger than for the other two iceberg shapes.

Larger errors are produced by the triangular iceberg using surface currents, since both pdf's show a similar right tail. Using the surface current results on one hand in smaller errors than with the other iceberg shaped, but on the other hand, it produces also the largest errors.

It is clearly visible in Fig. 10c and Fig. 10d that it is beneficial to exclude the wave force and Coriolis force. The problem with the wave force is that the simulated iceberg overshoots into north and east direction. If the wave force is excluded the northerly component is hindcasted well (Fig. 9) while the simulated iceberg does not drift far enough in east direction.

If the triangular shaped iceberg keel is excluded from the analysis and only the rectangular and elliptic shaped iceberg keels are considered the right tail of the pdf is similar for all considered current inputs, while the surface current produces a smaller mean error.

The pressure gradient force has only a small influence on the root-mean square error and the pdf's are almost on top of each other. If the wave, Coriolis and pressure gradient forces are excluded, the resulting pdf of the mean square error has the smallest mean error and a relatively small variance.

Iceberg Trajectory Summary

Even though only one iceberg trajectory was studies, this section illustrated how sensitive the dynamic iceberg model is to changes in the inputs and assumptions about the iceberg keel shape. The root mean square error varies from 178 m to 1741 m, with a mean error of 791 m. The final distance between simulated and observed iceberg trajectory varies between 180 m to 3376 m, with a mean final error of 1447 m. This variation was achieved without varying the mass or the drag coefficients of the iceberg. By not using presumably relevant information such as wave, Coriolis or pressure gradient force, the mean root mean square error and the mean final error can be reduced to 641 m and 1080 m. Even though the current, wind and waves were measured directly at the iceberg position, it is difficult to hindcast the iceberg trajectory with the measured forces. Furthermore, it is not necessarily advantageous to include more forces to the dynamical model, since they do not necessarily improve the hindcast result. Moreover, a simple kinematic model, which just considers the mean current velocity and a 2 % deflection by the wind, produces a similar result as the best dynamic model (Fig. 11). The root mean square error of the kinematic model is 140 m and the final error 187 m.

ESTIMATION OF THE ICEBERG GEOMETRY

Even though the previous section indicates that the dynamic model does not necessarily result in a good iceberg drift hindcast and is here even outperformed by a simple kinematic model, it describes the physics of the process more accurately than the kinematic model. If the current is measured close to the iceberg
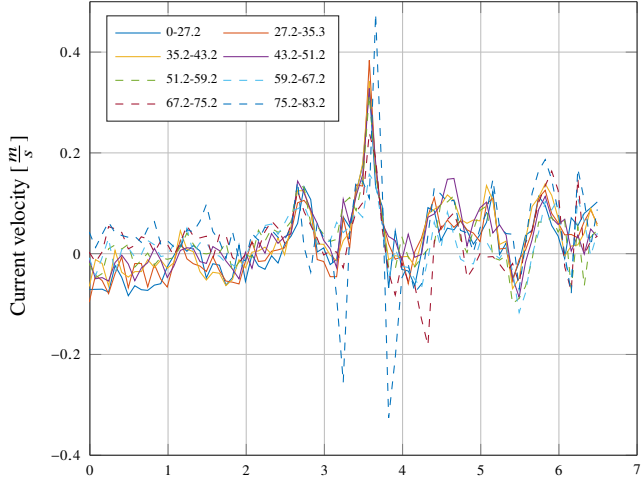
(a) NORTH-SOUTH VELOCITY
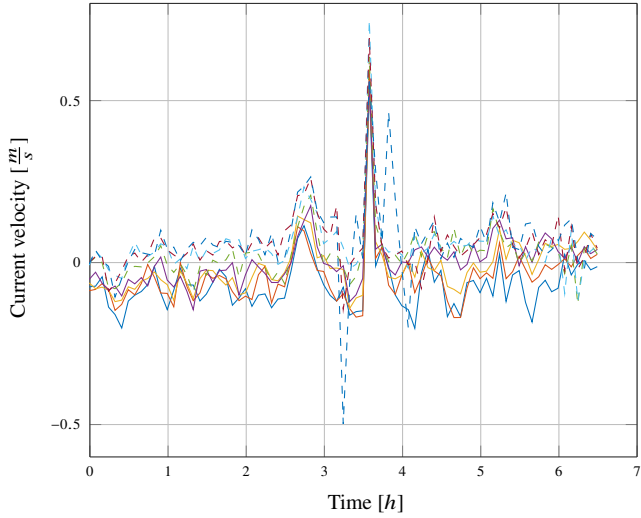
(b) EAST-WEST VELOCITY

FIGURE 5: CURRENT VELOCITIES IN DIFFERENT LAYERS (LAYERS UNDERNEATH SURFACE ARE GIVEN IN [M])

FIGURE 6: SIGNIFICANT WAVE HEIGHT (BLUE, SOLID) AND AVERAGE DIRECTION (ORANGE, DASHED).

FIGURE 7: FORCING ON ICEBERG.

for some time, it should be possible to estimate the scaled iceberg shape. The scaling is introduced by the drag coefficient. This is only possible if some confidence exist that the current input to the dynamic model is approximately correct. If this is not the case, the current input is more strongly corrected than the shape and drag coefficients [24]. Such an iceberg shape estimation can reduce the uncertainty in the shape parameters and reduce forecast errors in the iceberg prediction.

The iceberg geometry model

Additional information in form of constraints in the estimation process usually improves the estimation results, since the parameter space is reduced. Therefore, several constraints are introduced.
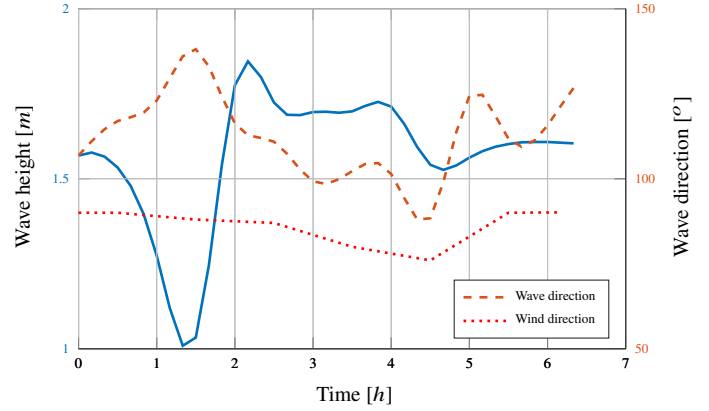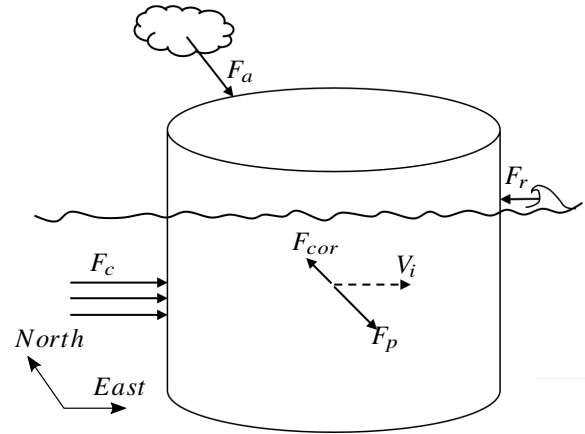
The radii of the iceberg shape are constrained to positive numbers. Moreover, the change of the radii is constrained. They have to decrease from the middle of the iceberg height. From several 3D iceberg profiling projects [25] it was shown that icebergs often have a shoulder. Therefore, the first radius was constrained to be within 75 % to 120 % of the sail length. The radius can decrease, since the first layer, if SADCP is used, is quite deep such that a decrease must be possible. The shoulder on the other hand may cause an increase of the radius.

Based on Archimedes law the overall mass and keel volume can be calculate if the sail volume of the iceberg is known

$$V_{keel} = V_{sail} \frac{\rho_{ice}}{\rho_w - \rho_{ice}}, \tag{3a}$$

$$m = (V_{sail} + V_{keel})\rho_{ice} = \left(1 + \frac{\rho_w}{\rho_w - \rho_{ice}}\right)V_{sail}\rho_{ice}. \tag{3b}$$
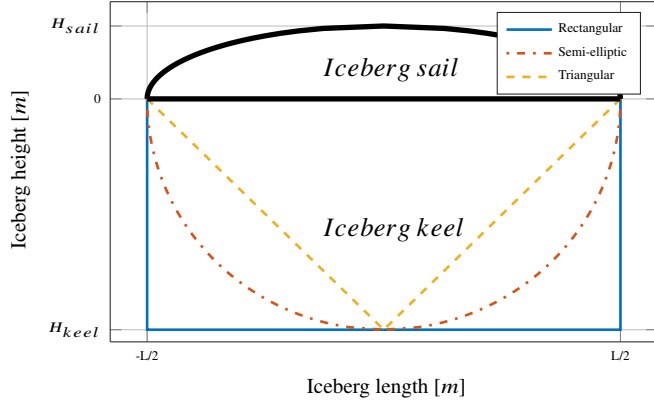
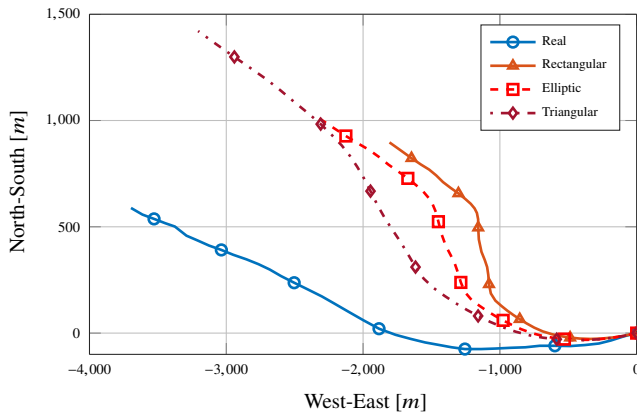**FIGURE 8**: ICEBERG KEEL GEOMETRIES

FIGURE 9: ICEBERG TRAJECTORY FOR DIFFERENT ICEBERG KEEL ASSUMPTIONS.

The sensitivity of Eqn. (3b) to changes of the iceberg density is high. A change of about 1 % in iceberg density causes a 8 % change in estimated iceberg mass and keel volume. Nonetheless, the estimated keel volume can be used with an idealized iceberg geometry assumption to constrain the overall keel volume. In this article, a cylindrical and elliptical iceberg geometry is considered (Fig. 12).

Cylindrical iceberg geometry. The volume of each layer can be calculated with

$$V_i = \pi r_i^2 h_i, \tag{4}$$

where r_i is the radius of the layer and h_i is the layer height. The sum of the volumes have to be the same as the estimated keel volume. The cross sections of each layer can be calculated with
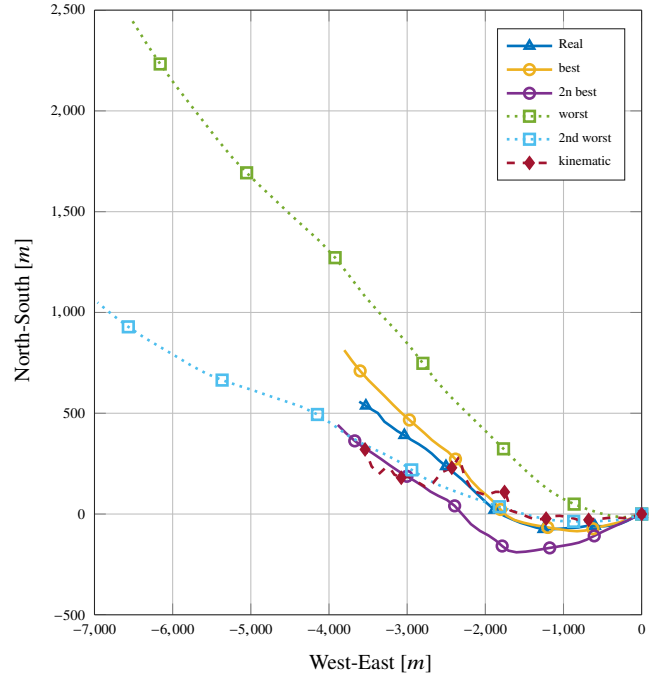
$$A_i = 2r_i h_i. \tag{5}$$

FIGURE 11: ICEBERG TRAJECTORIES FOR THE DYNAMIC MODEL (TWO BEST AND TWO WORST) AND THE TRAJECTORY OF THE KINEMATIC MODEL.
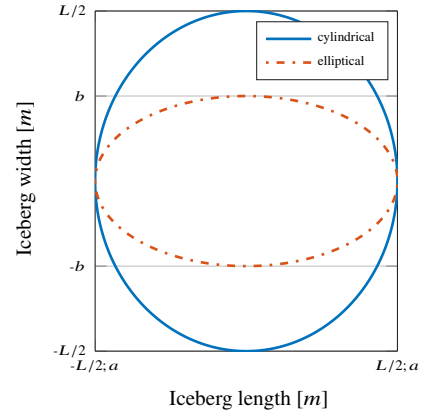

FIGURE 12: CYLINDRICAL AND ELLIPTICAL ICEBERG GEOMETRY SEEN FROM ABOVE.

Elliptical iceberg geometry. The radius of the ellipse changes with the angle of attack of the forces. The radius can be calculated by

$$r(\theta) = \frac{ab}{\sqrt{(b\cos\theta)^2 + (a\sin\theta)^2}}, \tag{6}$$

where θ is the angle between current direction and alignment of the major axis a of the ellipse. The minor axis is b. Con-

7

sequently, the alignment of the iceberg has to be known. The volume of each elliptic layer can be calculated by

$$V_i = \pi a_i b_i h_i. \tag{7}$$

For simplicity it was assumed that the ratio between major and minor axis is the same in each layer, such that

$$b_i = k a_i \tag{8}$$

holds, where k is the fixed ratio. The ratio k can be either estimated together with the layer radii or it can be fixed based on the sail geometry. If the ratio k is estimated, it is constrained to be within 0.3 to 1. Furthermore, it is assumed that the major and minor axis in each layer are aligned. As a result, the estimation problem for the elliptical shaped iceberg has the same amount of parameters or one parameter more as the estimation problem for the cylindrical shaped iceberg. The cross section area in each layer of the elliptical iceberg geometry can be calculated by

$$A_i = 2r_i(\theta)h_i. \tag{9}$$

Estimation algorithm

The iceberg geometry is estimated by a constrained least-squares parameter estimation algorithm. The discretization of the continuous time model (1) yields

$$x_{k+1} = f(x_k, u_k, p), \quad x_0 = x(t_0), \tag{10a}$$
$$y_k = h(x_k) + v_k, \tag{10b}$$

in which k denotes the samples taken at time t_k. The measurement noise $v_k \in \mathbb{R}^{n_y}$ is added to the measured outputs. The vector p represents the shape parameter that are estimated.

The following optimization problem is solved:

$$\min_{\{x_i, v_i, p\}} \sum_{i=0}^{N} \|y_i - h(x_i)\|_{R^{-1}}^2 \tag{11a}$$

$$s.t. \quad x_{i+1} = f(x_i, u_i, p) \quad \forall i = 0, ..., N-1$$
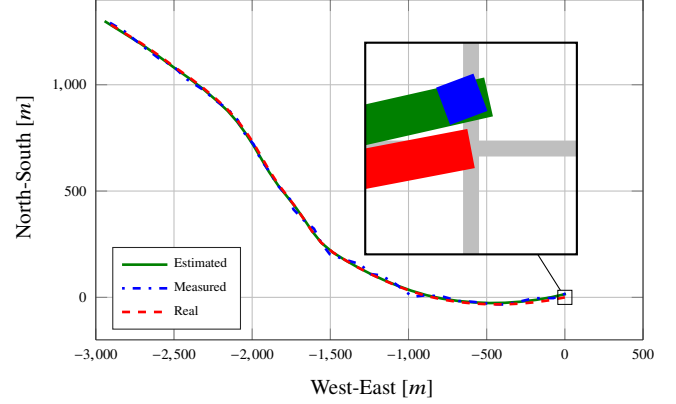$$x_i \in \mathbb{X}, \tag{11b}$$

FIGURE 13: ICEBERG DRIFT - ESTIMATION OF ICEBERG AREAS WITH MEASUREMENT NOISE ON ICEBERG POSITION (GAUSSIAN WHITE NOISE $\mu = 0$, $\sigma = 10$).

where $R \in \mathbb{R}^{n_y \times n_y}$, the measurement noise covariance matrix, is taken as the identity matrix. The set $\mathbb{X}$ is closed and convex, and usually given by a finite dimensional polyhedral set

$$\mathbb{X} = \{x_i \in \mathbb{R}^{n_x} | D_x x_i \le d_x\}, \tag{12}$$

where $D_x \in \mathbb{R}^{n_x \times n_x}$ is a matrix. The optimization problem is a constrained least squares problem for which standard literature to parameter estimation can be found [26].

Identifiability

Several simulation studies were performed to investigate if the parameters can be identified. The measured current, wind and wave forces were used to simulate the iceberg trajectory. If the simulated trajectory is used as position measurements without noise added, the geometry parameters can be identified perfectly. Under these noise free conditions, it is not necessary to include constraints to achieve perfect identification. However, if measurement noise in the position measurements or current measurements is added, the correct geometry can only be approximated. Problematic is that the iceberg drift trajectories are relative insensitive to changes in the iceberg geometry. An example of it is shown in Fig. 13. Even though the estimated and measured drift trajectories of the iceberg are almost identical, the error in the estimate of the cross section in comparison to the total cross section area is almost 35 %. Moreover, without constraints the estimated iceberg geometry becomes under noisy conditions quickly non-physical with, for example, layers in the middle of the iceberg keel that have a zero cross section area.

Since the sensitivity of the iceberg geometry to the iceberg drift trajectory is small, it is difficult to estimate the iceberg geometry without additional information. Therefore, to reduce the parameter space and improve the estimation results, it is necessary to introduce a geometry model of the iceberg (Fig. 14). In
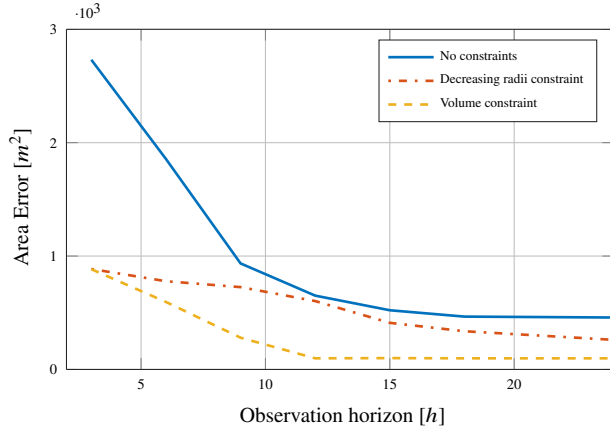
FIGURE 14: ERROR WITH DIFFERENT OBSERVATION HORIZONS AND CONSTRAINTS FOR A NINE LAYERED ICEBERG KEEL

FIGURE 15: ICEBERG GEOMETRY ESTIMATES FOR DIFFERENT INPUT SIGNALS (W:WAVE FORCE, P:PRESSURE GRADIENT FORCE, C:CORIOLIS FORCE).

addition, the parameter identification reaches an acceptable result more quickly. This is important, since the time of a ship or other devise that can measure the current regime close to the iceberg is limited.

The Cramér-Rao bound [26], a lower bound on the identification error depends on the current regime and the noise level. If the current is similar in every current layer and does not change much during observations, the lower bound of the identification error is higher than in cases where the current regime changes strongly. In the first case the information in the observations is low while in the second case the information is higher which lowers the identification error.

If the observation horizon is short, it is usually only possible to estimate the axis that is perpendicular to the current drift direction, since the current regime does not change much and the iceberg only rotates slightly.

Geometry estimation

The iceberg keel geometry is estimated for different input signals. Based on the observation of the iceberg sail, the ratio k is set to be 0.35. Furthermore, it is tested how sensitive the shape estimation is to whether the wave input, pressure gradient and Coriolis forces are included or not. The manually observed wind input is used in all geometry estimations. The different combinations result in eight geometry estimates. Six geometry estimates are shown in Fig. 15. The overall iceberg geometry is similar even though different forces were included to the model. In almost every estimate, the iceberg layers from $-40\,\mathrm{m}$ to $-87\,\mathrm{m}$ have not shown changing radii. This is caused by the volume constraint Eqn. (3b) combined with too little excitation and a short observation horizon. Consequently, the estimation algorithm cannot well distinguished between current layers. The deepest layer of all these iceberg geometries is estimated to be zero. Hence, the keel depth is estimated slightly smaller than measured with the SX90 sonar.
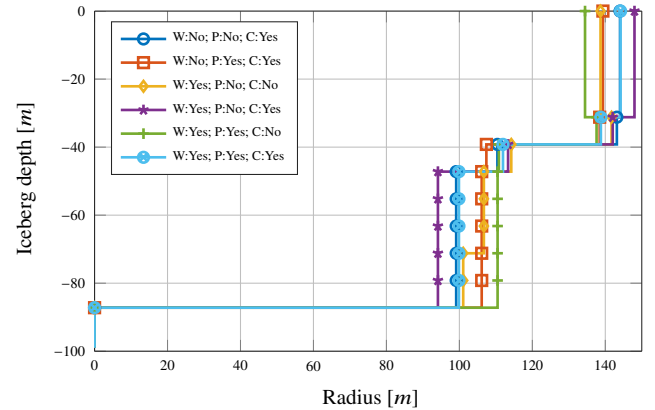
The root mean square error is about $150\,\mathrm{m}$ to $200\,\mathrm{m}$ if either wave force or Coriolis force is excluded from the model. If both forces are included, the root mean square error is about $580\,\mathrm{m}$.

The two geometries where wave and Coriolis force were excluded from the model, are not shown. They resulted in a non-physical iceberg geometry. The radii of second and third iceberg layers are in those cases estimated with zero length while the fourth layer has a large radius of about $250\,\mathrm{m}$. Since the change of the radii is only constrained from the middle of the iceberg height to the deepest layer, this non-physical iceberg shape is possible during estimation. Further constraints may remove this problem.

An increase of $10\,\%$ of the iceberg sail volume increases also the iceberg mass $10\,\%$. The radii in the iceberg geometry estimation increases as well, but the overall geometry stays similar to the original estimate. A similar effect has an about $1.5\,\%$ change of the ice density to which the iceberg mass is very sensitive.

CONCLUSION

The article showed data taken from one iceberg trajectory. Current, winds and waves were measured close to the iceberg. It was illustrated how sensitive the dynamic iceberg model is to parameter changes of the model. Moreover, for the considered iceberg track it was not necessarily beneficial to obtain detailed information about waves and currents at the iceberg position. In fact, the iceberg trajectory was also correctly hindcasted with surface current and no wave information. Even though, this might be an exception in this particular case, it shows that variance in the drift trajectories of the dynamic model is large, because of the many uncertain parameters in the model. In addition, it is not straightforward to include detailed information, for example, about the iceberg shape in the quite simplified dynamic iceberg

Copyright © 2017 by ASME

model. In contrast, a more detailed and complicated dynamic model increases the amount of parameters and most likely, as a consequence, the variance of the model.

Despite the problems with the dynamic model, it is possible to approximate the iceberg geometry with a simple parameter identification algorithm. Under the assumption that the dynamic iceberg model approximates the correct physical behavior of the process, the iceberg geometry can be estimated if the iceberg and current regime around the iceberg is observed for some time. This estimated iceberg geometry is adjusted to the dynamic iceberg model and can afterwards be used easily for iceberg drift forecasts. The iceberg geometry identification by the algorithm presented in this article can be improved by collecting more knowledge about iceberg profiles. This knowledge can be transformed in further constraints, which can be incorporated into the algorithm.

REFERENCES

[1] Smith, S. D., and Banke, E., 1981. "A numerical model of iceberg drift". In Proc. Port and Ocean Engineering under Arctic Conditions'81.

[2] EI-Tahan, M., EI-Tahan, H., Venkatesh, S., et al., 1983. "Forecast of iceberg ensemble drift". In Offshore Technology Conference.

[3] Bigg, G. R., Wadley, M. R., Stevens, D. P., and Johnson, J. A., 1997. "Modelling the dynamics and thermodynamics of icebergs". *Cold Regions Science and Technology, 26*(2), pp. 113–135.

[4] Kubat, I., Sayed, M., Savage, S. B., and Carrieres, T., 2005. "An operational model of iceberg drift". *International Journal of Offshore and Polar Engineering, 15*(2), pp. 125–131.

[5] Eik, K., 2009. "Iceberg drift modelling and validation of applied metocean hindcast data". *Cold Regions Science and Technology, 57*, pp. 67–90.

[6] Broström, G., Melsom, A., Sayed, M., and Kubat, I., 2009. Iceberg modeling at met.no: Validation of iceberg model. Tech. Rep. 17, Norwegian Meteorological Institute, Dec.

[7] Turnbull, I. D., Fournier, N., Stolwijk, M., Fosnaes, T., and McGonigal, D., 2015. "Operational iceberg drift forecasting in northwest greenland". *Cold Regions Science and Technology, 110*, pp. 1 – 18.

[8] Allison, K., Crocker, G., Tran, H., and Carrieres, T., 2014. "An ensemble forecast model of iceberg drift". *Cold Regions Science and Technology, 108*, pp. 1 – 9.

[9] Mountain, D., 1980. "On predicting iceberg drift". *Cold Regions Science and Technology, 1*(3-4), pp. 273 – 282.

[10] Smith, S. D., and Donaldson, N. R., 1987. *Dynamic modelling of iceberg drift using current profiles*. Fisheries and Oceans, Canada.

[11] McGuire, P., Younan, A., Wang, Y., Bruce, J., Gandi, M., King, T., Keeping, K., Regular, K., et al., 2016. "Smart iceberg management system–rapid iceberg profiling system". In Arctic Technology Conference.

[12] Bruce, J., Younan, A., MacNeill, A., et al., 2016. "Applications of iceberg profiling data to improve iceberg management success". In Arctic Technology Conference.

[13] Stuckey, P., Younan, A., Burton, R., Alawneh, S., et al., 2016. "Modelling iceberg-topsides impacts using high resolution iceberg profiles". In Arctic Technology Conference.

[14] King, T., Younan, A., Richard, M., Bruce, J., Fuglem, M., Phillips, R., et al., 2016. "Subsea risk update using high resolution iceberg profiles". In Arctic Technology Conference.

[15] Fuglem, M., Younan, A., et al., 2016. "A 3d time-domain model for iceberg impacts with offshore platforms and subsea equipment". In Arctic Technology Conference.

[16] Wang, Y., deYoung, B., Bachmayer, R., et al., 2015. "A method of above-water iceberg 3d modelling using surface imaging". In The Twenty-fifth International Offshore and Polar Engineering Conference, International Society of Offshore and Polar Engineers.

[17] Zhou, M., Bachmayer, R., deYoung, B., et al., 2016. "Adaptive heading controller on an underwater glider for underwater iceberg profiling". In Arctic Technology Conference.

[18] ArcticNet, 2004-2016. [Online]. Available: www.arcticnet.ulaval.ca.

[19] C-CORE, 2007. "Ice management for structures in sea ice with ridges and icebergs. volume 1 - state of the art in iceberg management". *C-CORE Report R-07-037-544*.

[20] Barker, A., Sayed, M., and Carrieres, T., 2004. "Determination of iceberg draft, mass and cross-sectional areas". In Proc. International Offshore and Polar Engineering Conference'04, Vol. 2, pp. 899–904.

[21] Sodhi, D., and Dempster, R., 1975. "Motion of icebergs due to changes in water currents". In Proc. OCEAN'75, pp. 348–350.

[22] Lichey, C., and Hellmer, H. H., 2001. "Modeling giant-iceberg drift under the influence of sea ice in the weddell sea, antarctica". *Journal of Glaciology, 47*(158), pp. 452–460.

[23] Andersson, L. E., Scibilia, F., and Imsland, L., 2016. "Estimation of systems with oscillating input - applied to iceberg drift forecast". In To appear in: IEEE Multi-conference on Systems and Control (MSC), International Conference on Control Applications (CCA), Buenos Aires.

[24] Andersson, L. E., Scibilia, F., and Imsland, L., 2016. "An estimation-forecast set-up for iceberg drift prediction". *Cold Regions Science and Technology, 131*, pp. 88–107.

[25] Younan, A., Ralph, T., Ralph, F., and Bruce, J., 2016. "Overview of the 2012 iceberg profiling program". In Arctic Technology Conference.

[26] Van Trees, H. L., and Bell, K. L., 2013. *Detection estimation and modulation theory, pt. I.* Wiley.